arXiv:1606.07969v1 [cond-mat.stat-mech] 25 Jun 2016

Percolation of overlapping squares or cubes on a lattice

Zbigniew Koza, Grzegorz Kondrat, and Karol Suszczyński

Faculty of Physics and Astronomy, University of Wrocław, 50-204 Wrocław, Poland

E-mail: zbigniew.koza@ift.uni.wroc.pl

Abstract. Porous media are often modelled as systems of overlapping obstacles, which leads to the problem of two percolation thresholds in such systems, one for the porous matrix and the other one for the void space. Here we investigate these percolation thresholds in the model of overlapping squares or cubes of linear size $k > 1$ randomly distributed on a regular lattice. We find that the percolation threshold of obstacles is a nonmonotonic function of k, whereas the percolation threshold of the void space is well approximated by a function linear in $1/k$. We propose a generalization of the excluded volume approximation to discrete systems and use it to investigate the transition between continuous and discrete percolation, finding a remarkable agreement between the theory and numerical results. We argue that the continuous percolation threshold of aligned squares on a plane is the same for the solid and void phases and estimate the continuous percolation threshold of the void space around aligned cubes in a 3D space as 0.036(1). We also discuss the connection of the model to the standard site percolation with complex neighborhood.

PACS numbers: 64.60.ah, 61.43.Gt

Submitted to: *J. Stat. Mech.*

Keywords: Percolation threshold; continuous percolation; finite-size scaling; excluded volume theory; critical exponents

1. Introduction

One of the standard ways of constructing a nontrivial model of a heterogeneous porous material is to fill the space randomly with a number of identical impermeable objects that are free to overlap [1]. Models of this type can be used to derive exact bounds on the values of various transport coefficient, including the effective diffusion coefficient, electrical conductivity, dielectric constant and magnetic permeability of dispersions [2, 3], whereas at high obstacle concentrations they can be used to model consolidated porous media, e.g., sandstones, sintered materials, rocks, or complex catalysts [1, 4, 5, 6].

Systems of identical overlapping objects are often described with the reduced number density $\eta = vN/V$, where v is the area (or volume) of each object, N is their number, and V is the system volume [7]. As η is gradually increased from 0, the system undergoes two critical transformations. The first one is related to the connectivity of the solid phase formed by the obstacles: at low densities the obstacles form a disconnected phase, whereas above a critical value η_s this phase becomes connected. The second one is related to the connectivity of the void space: above some $\eta_\mathrm{v} \geq \eta_\mathrm{s}$ the void space becomes disconnected and the transport is blocked. Clearly, η_s and η_v can be identified as the percolation thresholds for the solid and the void phase, respectively.

So far a vast majority of research has focused on the simplest case of spherical obstacles. Spheres (in 3D) and disks (in 2D) are particularly convenient in the mathematical treatment of problems where the transport is governed by the Laplace's equation, e.g., diffusion [2]. The task of determining η_s is then equivalent to the well known problem of finding the percolation threshold for overlapping spheres [8, 9] or disks [8, 9, 10, 11]. Similarly, the value of η_v can be identified as the percolation threshold in the "Swiss-cheese" model for spheres [12, 13, 14] or disks [14, 15], in which percolation is sought for in the void phase.

However, other shapes are also important [16], e.g., needles [10, 11, 17, 18], fibers [17], ellipses [19], and ellipsoids [20]. In particular, many computer simulations discretize the space into a regular lattice and model a porous medium using overlapping cubes [21, 22] or squares [23, 24, 25, 26]. Therefore we investigate the problem of the percolation thresholds in the model of overlapping squares (2D) or cubes (3D) on a regular lattice, focusing on their dependence on the size of the obstacles. While one might expect that the values of both percolation thresholds for finite values of the obstacle size k could be approximated by interpolating their values between the well known cases of $k = 1$ (standard site percolation on a lattice) and $k \to \infty$ (off-lattice percolation of freely overlapping squares or cubes), we found that this is not the case and the percolation threshold of the obstacles exhibits a maximum at a finite value of $k > 1$. This result is particularly important for designing numerical models of porous media close to percolation.

By investigating the limit of $k \to \infty$, the model studied here can be used to explore the transition between discrete and continuous percolation. On the other hand, the dependency of continuous percolation on the obstacle shape can be investigated with a

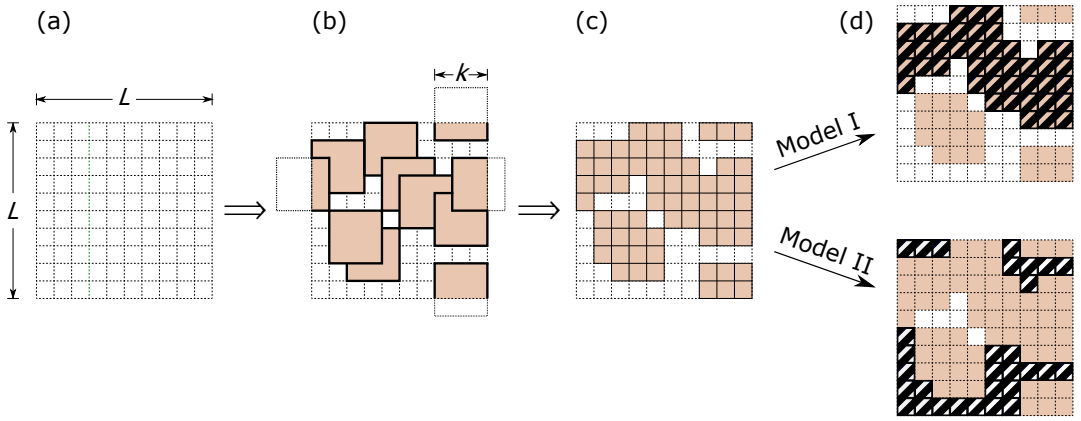

Figure 1. Construction of the models. An empty regular lattice of size $L \times L$ lattice units (l.u.) with periodic boundary conditions (a) is filled at random with square obstacles of size $k \times k$ l.u. aligned to the lattice axes (b) and the elementary cells occupied by the obstacles are identified (c); finally, the problem is reduced to the site percolation through the occupied or unoccupied elementary cells in Model I and Model II, respectively (d). The same method was also used in three dimensions.

simple theory, the excluded volume approximation [27, 16]. We combine the two facts and generalize the excluded volume theory to discrete systems, finding a remarkably good agreement with numerical results for all obstacle sizes k. By extrapolating the numerical results obtained for discrete systems, we improve the accuracy of the determination of the continuous percolation threshold of aligned, overlapping cubes in three dimensions as well as provide the values of continuous percolation thresholds of the void space around aligned squares and cubes in dimensions two and three. Moreover, we show that a direct relation between the model of overlapping objects of arbitrary shape and the standard site percolation with complex neighborhood can be used to improve the accuracy of the percolation threshold determination in a class of percolation models.

2. The Model

As illustrated in figure 1, we consider a square (2D) or cubic (3D) lattice of linear size L lattice units, on which square or cubic "obstacles" of linear size k lattice units are deposited at random, where k, L are some integer parameters, $1 \leq k \ll L$, and the periodic boundary conditions are imposed on the system during the obstacle deposition to reduce the finite-size effects [28, 29]. The obstacles are aligned to the underlying lattice, their edges coinciding with lattice nodes, and are free to overlap. The volume occupied by obstacles is thus a simple union of elementary lattice cells and the model is essentially discrete. Henceforth the volume occupied by obstacles shall be called phase A or solid phase, whereas the remaining volume shall be called phase B or void phase.

We investigate two cases, which will be denoted as Model I and Model II. In Model I we consider the percolation of obstacles, whereas in Model II we consider the percolation of the void space. Two elementary cells are considered to be connected

directly if and only if they belong to the same phase and share the same side (2D) or face (3D). We define a percolation cluster as a set of elementary cells spanning two opposite system sides through a sequence of directly connected elementary cells. Thus, Model I interpolates between the standard model of site percolation on a regular lattice ($k = 1$) and the model of continuous percolation of aligned squares [7, 18] or cubes [7] ($k \to \infty$). Similarly, Model II interpolates between the site percolation of voids on a regular lattice ($k = 1$) and the continuous percolation of voids around aligned squares or cubes ($k \to \infty$).

We shall express the percolation threshold in terms of the porosity, φ, which is one of the most fundamental concepts in porous media studies. In both Model I and II the porosity is defined as the ratio of the volume occupied by phase B (void space) to the system volume. For Model II this quantity is equivalent to the so called remaining area/volume fraction [19], whereas $\varphi = 1 - p_{\mathrm{A}}$ for model I, with p_{A} being the area (2D) or volume (3D) fraction of phase A.

Since locations of each obstacle are random and mutually independent, and since the porosity can be identified with the probability that an elementary cell is unoccupied by any obstacle, the expected porosity, $\langle\varphi\rangle$, can be expressed as

$$\langle\varphi\rangle = (1 - v/V)^N = (1 - \eta/N)^N. \tag{1}$$

This formula can be used to generate a system of a given porosity; it also implies that

$$\varphi = \exp(-\eta) \tag{2}$$

at the thermodynamic limit [7].

3. Numerical and mathematical details

To find the percolation thresholds we used two independent computer programs. One of them keeps track of whether each elementary cell belongs to phase A or B. In this approach the execution time of each simulation is $\propto L^d$, where d is the space dimensionality, and we were able to run it for $L \leq 4096$ ($d = 2$) and $L \leq 1024$ ($d = 3$). We used this program to simulate Model II (percolation of voids).

The second program uses data structures typical of the algorithms designed for the continuous percolation: each obstacle is identified by its coordinates, i.e., by only d integers, and the clusters are found using the union-find algorithm. In this case the computer memory storage, as well as the simulation time of each percolation cluster, is $\propto (L/k)^d$ and we were able to run the program for $L/k \leq 5000$ ($d = 2$) and $L/k \leq 400$ ($d = 3$). While the second program allows for much larger system sizes L, it cannot be efficiently used for Model II. We used it to simulate Model I (percolation of obstacles).

In each case we assumed periodic boundary conditions in the direction(s) perpendicular to the direction along which we sought the percolation. The number of independent samples (N) varied from 10^7 for very small systems to 10^3 for larger L so as to ensure that we can determine the percolation threshold for given values of L and k with the absolute accuracy of at least 5×10^{-5}. To this end we determined the

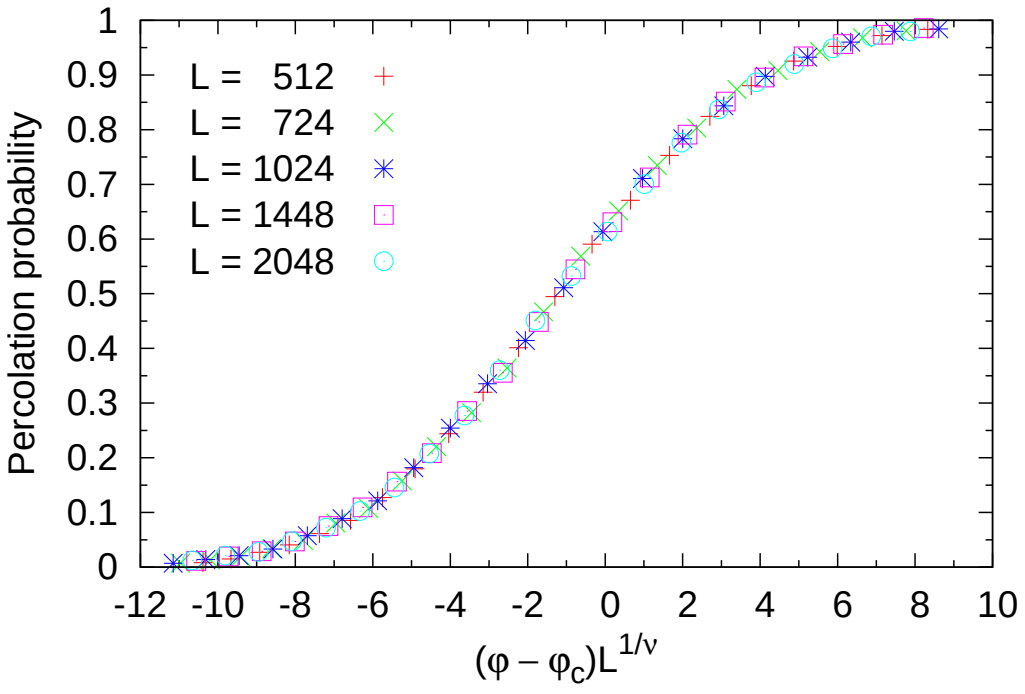

Figure 2. The data collapse according to the universal scaling, equation (3) with $\varphi_k^{\mathrm{c}} = 0.3505$, $\nu = 4/3$, obtained for Model II with the obstacle size $k = 20$ and space dimension $d = 2$.

probability $P_{L,k}(\varphi)$ that a system of size L, obstacle size k, and porosity φ contains a percolating (spanning) cluster. In accordance with the finite-size scaling theory, $P_{L,k}$ is expected to scale with L and the deviation $\varphi - \varphi_k^{\mathrm{c}}$ from the critical porosity φ_k^{c} as [28, 30]

$$P_{L,k}(\varphi) = f_k\left((\varphi - \varphi_k^{\mathrm{c}})L^{1/\nu}\right), \quad L/k \gg 1, \tag{3}$$

where ν is the correlation length exponent and f_k is a scaling function, cf. figure 2. Then we define an effective, L-dependent critical porosity $\varphi_k^{\mathrm{c}}(L)$ as the solution to $P_{L,k}(\varphi) = 0.5$. This value can be obtained, for example, by fitting the data to a curve with a similar, sigmoidal shape, e.g.,

$$P_{L,k}(\varphi) \approx \frac{\mathrm{erfc}\{[\varphi_k^{\mathrm{c}}(L) - \varphi]/\Delta(L)\}}{2}. \tag{4}$$

Not only does this method provide an accurate estimation of $\varphi_k^{\mathrm{c}}(L)$, but it also yields the width of the percolation transition, $\Delta(L)$, which can be used to estimate the value of the critical exponent ν from

$$\Delta(L) \propto L^{-1/\nu}, \quad L \gg 1. \tag{5}$$

Once $\varphi_k^{\mathrm{c}}(L)$ have been determined for sufficiently large values of L, they can be used to obtain the critical porosity φ_k^{c} from

$$\varphi_k^{\mathrm{c}}(L) - \varphi_k^{\mathrm{c}} \propto L^{-1/\nu}, \quad L \gg 1. \tag{6}$$

4. Results

4.1. Asymptotic regime and exponent ν

The critical porosity can be determined from (6) by fitting $\varphi_k^{\mathrm{c}}(L)$ to a nonlinear function $\varphi_k^{\mathrm{c}} + aL^{-1/\nu}$ with three fitting parameters, φ_k^{c}, a and ν. The fourth unknown parameter, $L_{\min}$ is the minimum value of L for which the asymptotic regime expressed by (6) holds with a sufficient accuracy. However, the value of the critical exponent ν is expected to be universal, k-independent. We verified this hypothesis positively for Models I and II in dimensions 2 and 3 for all tested values of k using both (5) and (6) (data not shown). Therefore in the fitting procedure we reduced the number of unknowns to two, assuming the most accurate value of the thermal exponent $y_{\mathrm{t}} = 1/\nu$ available for the standard site percolation, $1/\nu = 3/4$ and 1.141 for $d = 2$ and 3, respectively [31, 32]. The value of $L_{\min}$ was determined by requiring that the reduced chi-squared statistic of the fit is $\sim O(1)$ and neither this parameter nor the estimated value of the critical porosity varies significantly for $L > L_{\min}$. For Model I we found $L_{\min} = 100k$ and $60k$ for $d = 2$ and 3, respectively, whereas for Model II we found $L_{\min} = 50k$ for $d = 2, 3$. The accuracy of our data was insufficient for application of fits with higher-order terms, a standard technique for simpler models of percolation [31, 32].

Selected results showing the convergence of the effective critical porosity to its asymptotic value are depicted in figure 3. As can be seen, the convergence rate is similar for different values of k.

4.2. Critical porosity

4.2.1. Model I The critical porosity for Model I (percolation of obstacles) for several values of k ranging from 1 to 10 000 is listed in table 1, and its dependency on $1/k$ in two and three dimensions is depicted in figure 4. A striking feature of these results is a nonmonotonic dependency of φ_k^{c} on k. This effect is particularly strong in three dimensions—in this case the maximum value of the critical porosity is located at $k = 3$ and exceeds its value for the standard site percolation ($k = 1$) by $\approx 10\%$.

Our results are in agreement with those obtained for $k = 1$ (standard site percolation) in references [33, 31]. Moreover, they allow to estimate the critical porosity in the limit of $k \to \infty$, which corresponds to the continuous percolation of aligned squares or cubes. To this end we assumed that φ_k^{c} depends linearly on $1/k$ for sufficiently large k and hence the value of $\varphi_\infty^{\mathrm{c}} = \lim_{k\to\infty} \varphi_k^{\mathrm{c}}$ can be estimated through linear extrapolation. The critical surface/volume Φ_{c} of the continuous percolation is then related to the critical porosity through $\Phi_{\mathrm{c}} = 1 - \varphi_\infty^{\mathrm{c}}$. Our result for $d = 2$, $\Phi_{\mathrm{c}} = 0.66675(2)$, agrees with the value 0.66674349(3) obtained by Mertens and Moore [18]. For the case $d = 3$ we obtained $\Phi_{\mathrm{c}} = 0.27727(2)$, which is an improvement over the value 0.2773(2) reported by Baker et al. [7].

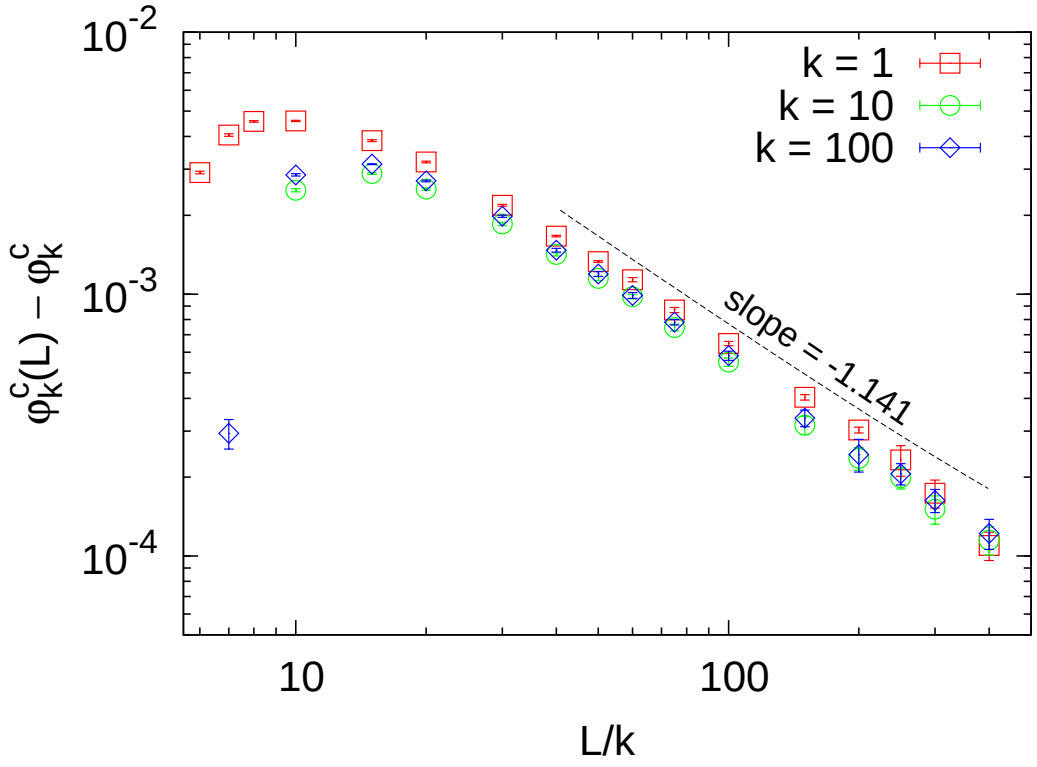

Figure 3. (Color online) Convergence of the effective critical porosity $\varphi_k^c(L)$ to its asymptotic value φ_k^c for Model I in three dimensions and $k = 1, 10, 100$. The dashed line is a guide to the eye with the slope $-1/\nu = -1.141$ determined for the standard site percolation ($k = 1$, $d = 3$) in Ref. [31, 32].

Table 1. Critical porosity for selected values of k. The values for $k \to \infty$ come from extrapolation and are expected to be the same for $d = 2$. The data for Model II and $k > 20$ are not available.

k	Model I		Model II	
	$d = 2$	$d = 3$	$d = 2$	$d = 3$
1	0.40726(1)	0.68840(1)	0.5926(2)	0.3117(1)
2	0.41635(2)	0.76013(2)	0.4868(1)	0.1687(1)
3	0.40414(2)	0.76564(1)	0.4417(1)	0.1195(1)
4	0.39352(1)	0.76362(1)	0.4172(2)	0.0961(1)
5	0.38533(2)	0.76044(2)	0.4015(2)	0.0829(2)
7	0.37403(1)	0.75450(1)	0.3829(3)	0.0685(2)
10	0.36391(2)	0.74803(1)	0.3683(5)	0.0585(3)
20	0.34994(2)	0.73754(2)	0.351(1)	0.048(1)
100	0.33682(2)	0.72611(1)	—	—
1 000	0.33361(1)	0.72306(2)	—	—
10 000	0.33326(1)	0.72277(2)	—	—
∞	0.33325(2)	0.72273(2)	0.334(1)	0.036(1)

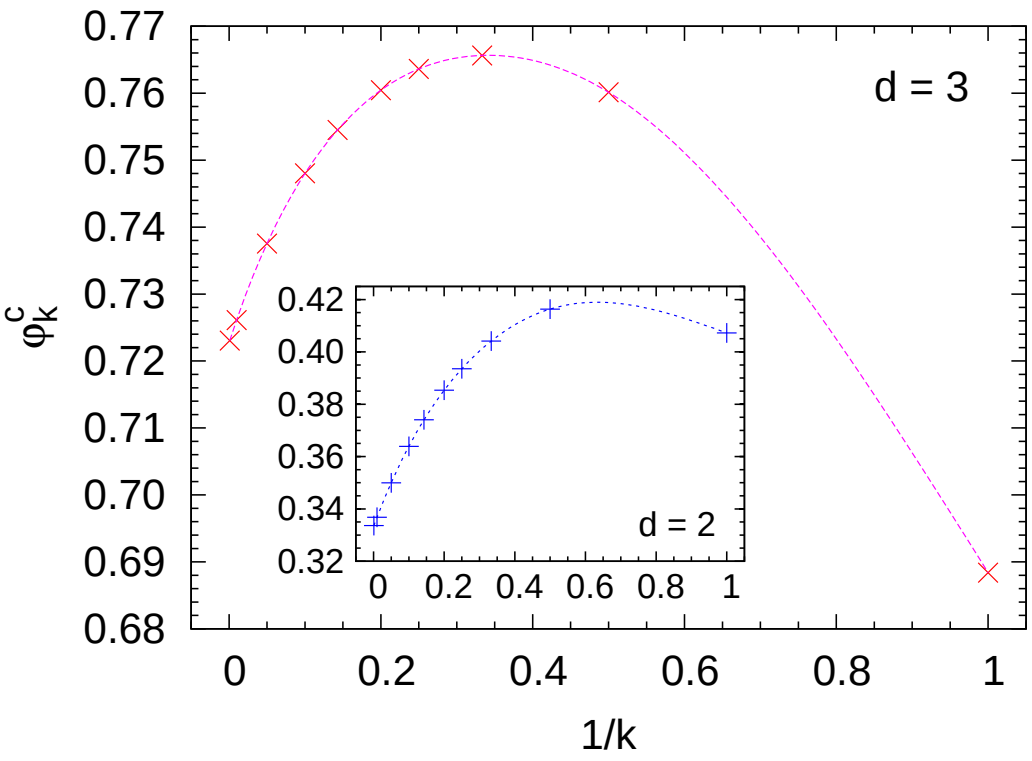

Figure 4. (Color online) Critical porosity φ_k^c for Model I in 3D as a function of the reciprocal of the obstacle size, $1/k$. The dashed line is a guide to the eye drawn with cubic splines. Inset: the same for $d = 2$.

4.2.2. Model II The critical porosity obtained for Model II (percolation of voids) is listed in table 1, and figure 5 shows that its dependency on $1/k$ is almost linear both for $d = 2$ and $d = 3$. We verified that our results for $k = 1$ are in agreement with those reported recently in [33, 31]. As for the limit of $k \to \infty$, which corresponds to the continuum percolation of voids, this problem is much harder than the continuous percolation of obstacles and most of the research has been concentrated on overlapping discs or spheres. Our results suggest that in this limit the critical porosities for Models I and II are the same if $d = 2$. This can be justified as follows. Consider two obstacles that are close to each other. As shown schematically in figure 6, if they overlap or share a side (2D) or face (3D), they facilitate the percolation of obstacles (Model I). If they are disjoint, they facilitate percolation of the void phase (Model II). However, if they touch only at a corner (2D) or an edge (3D), they block the percolation of both phases. The latter case is very common if k is small, but the probability of two squares sharing only a corner or two cubes sharing only an edge quickly decreases as $k \to \infty$. Thus, for continuous percolation the situation depicted in figure 6b practically does not occur and its impact is negligible. This implies that either phase A or B percolates regardless of the porosty. As the percolation in one direction of a 2D system precludes the percolation of the other phase in the perpendicular direction, and since the system is isotropic, the

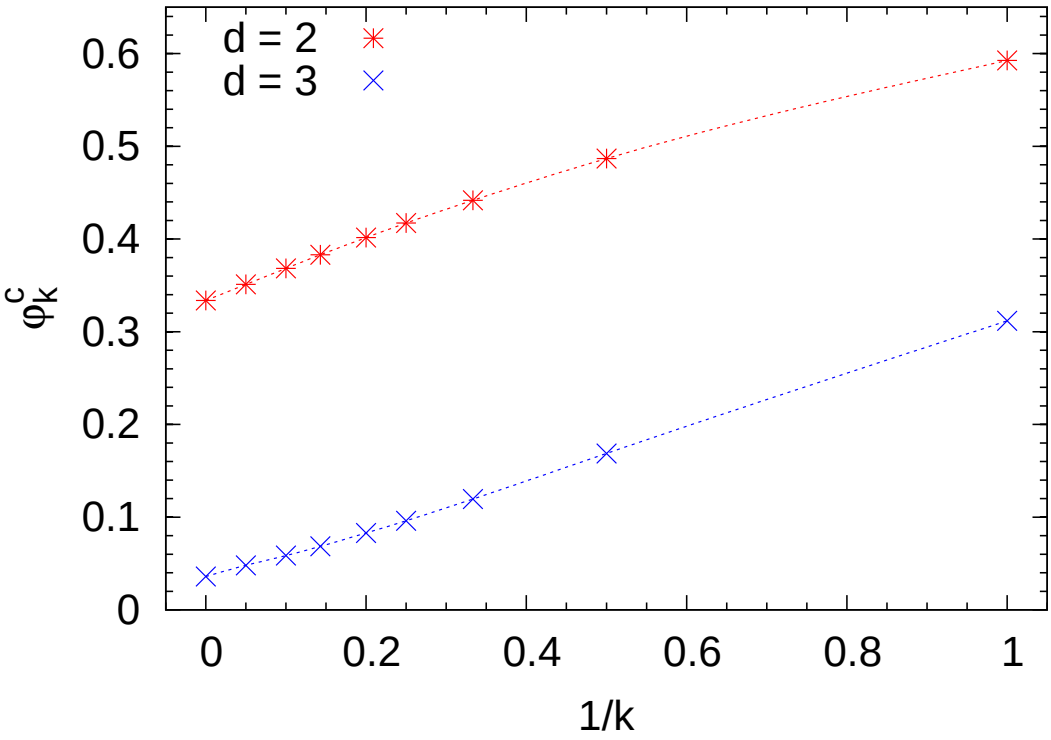

Figure 5. (Color online) Critical porosity φ_k^c for $d = 2, 3$ as a function of the reciprocal of the obstacle size, $1/k$, for Model II (percolation of voids). The values at $1/k = 0$ come from extrapolation. The dashed lines are guides to the eye drawn with cubic splines.

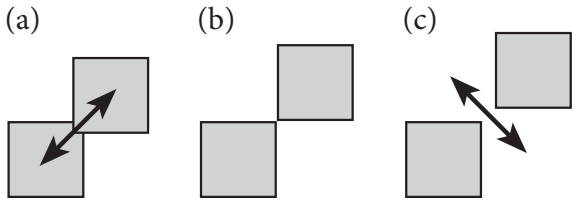

Figure 6. (a) Overlapping squares contribute to percolation of obstacles. (b) Two squares touching only at the corners block percolation of both phases. (c) Two disjoint squares facilitate percolation of the void phase.

continuous percolation thresholds of aligned squares of the obstacles (Model I) and of the void space around them (Model II) must be the same. Consequently, even though our direct estimation of φ_∞^c in Model II yields 0.334(1), one can safely use its more accurate approximation for Model I, 0.33325651(3) [18].

For $d = 3$ the critical porosity in Model II is always smaller than in Model I, which means that for any k, including the case $k \to \infty$, there exists a range of porosities for which the system resembles a sponge: both the solid and void phases percolate.

Moreover, the value of φ_k^{c} for $k \to \infty$ turns out to be close to the critical porosity 0.0317 of the void space around overlapping spheres [13] (see also [14]). As expected, for $d = 2$ we found the opposite behavior: it is impossible to have a two-dimensional, infinite system with percolation of both phases. Instead, for any finite k there exists a range of porosities for which neither phase percolates. The width of this range shrinks to zero as $k \to \infty$. Note that our result for $k \to \infty$, $\varphi_\infty^{\mathrm{c}} \approx 0.33324$, is much larger than 0.159 reported by van der Marck [14] for continuous percolation of the void phase around disks. Such a large discrepancy cannot be explained by the difference in the shape of obstacles. As Marck's result is also smaller than the critical porosity of disks, $\varphi_\infty^{\mathrm{c}} \approx 1 - 0.67634831 \approx 0.32$ [18], his result is probably erroneous.

4.3. Discrete excluded volume approximation for Model I

According to the excluded volume theory [27, 16], the continuum percolation threshold for overlapping obstacles can be approximated with

$$n_{\mathrm{c}} V_{\mathrm{ex}} \approx B, \tag{7}$$

where $n_{\mathrm{c}} = \eta_{\mathrm{c}}/v$ is the critical number density of objects, V_{ex} is their excluded area or volume, and B is the average number of overlaps per obstacle at criticality. In continuous percolation V_{ex} is defined as the area (volume) around an object into which the center of another similar object is not allowed to enter if overlapping of the two objects is to be avoided. Consequently, V_{ex} can be interpreted as a measure of the rate at which consecutive obstacles, which are free to overlap, form new connections as they are being placed in the system. Therefore, for discrete models we define V_{ex} as the number of obstacle configurations which make a connection with a given obstacle. In other words, for discrete models V_{ex} should be regarded as a "connectedness factor" rather than the excluded volume. For Model I this leads to $V_{\mathrm{ex}}(k)$ being the number of elementary lattice cells in a square or cube of length $2k + 1$ that are not at its corners ($d = 2$) or edges ($d = 3$). A general formula for $V_{\mathrm{ex}}(k)$ in Model I reads

$$V_{\mathrm{ex}}(k) = (2k - 1)^{d-1}(2k + 2d - 1). \tag{8}$$

Combining equations (2) and (7) one arrives at a general relation for the critical porosity

$$\varphi^{\mathrm{c}} \approx \exp\left(-B\frac{v}{V_{\mathrm{ex}}}\right). \tag{9}$$

For Model I it reduces to

$$\varphi_k^{\mathrm{c}} \approx \exp\left[-B_d \frac{k^d}{(2k-1)^{d-1}(2k+2d-1)}\right], \tag{10}$$

where B_d is the B factor for the space dimension d.

The ratio V_{ex}/v is nonmonotonic in k, with the maximum at a non-integer

$$k^{\max} = d - 1/2. \tag{11}$$

This corresponds to the nonmonotonic dependency of the critical porosity on the obstacle size seen in figure 4 for $d = 2, 3$.

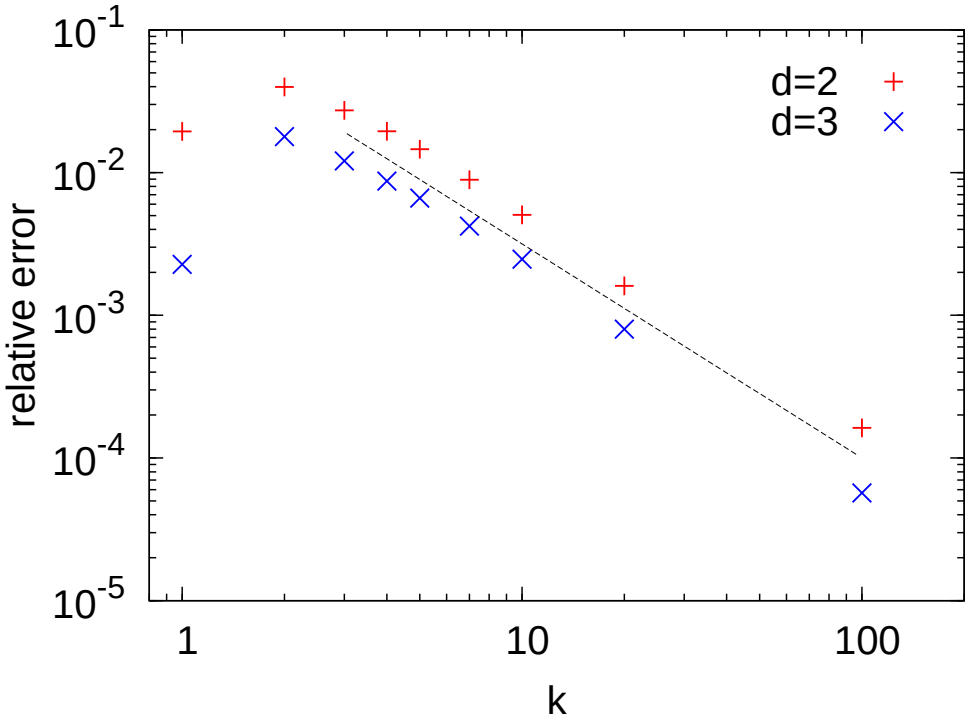

Figure 7. (Color online) The relative error of the critical porosity, φ_k^{c}, approximated with equation (10), as a function of the object size k, for $d = 2, 3$ (Model I). The simulation results (table 1) were assumed to be the true values and B_d was taken from the continuous percolation. The dashed line is a guide to the eye with the slope $-3/2$.

Parameters B_d in (10) can be treated as fitting parameters to the simulation data or can be obtained independently using other methods. In the former case we found that $B_2 = 4.49$, $B_3 = 2.67$ and φ_k^{c} determined from equation (10) agree with the simulation results within 2 significant digits (the absolute error < 0.01) for all k. In the later case one can use the values for the continuous percolation: $B_2 = 4.3953711(5)$ and $B_3 = 2.5978(5)$. They can be obtained by inserting the most accurate values of the critical porosity into

$$B_d = -2^d \ln \varphi_\infty^{\mathrm{c}}, \tag{12}$$

which follows immediately from (9) if we assume this relation to be exact. These values agree with $B_2 = 4.39(1)$ and $B_3 = 2.59(1)$ reported in [7].

The error introduced by (10) can be estimated using the simulation results as the reference values. As shown in figure 7, even with the values of B_d taken from the continuous percolation, the accuracy of (10) is remarkable. As expected, the quality of (10) improves as k goes to infinity. It is rather surprising that the correction to (10) scales in the same way, as $k^{-3/2}$, for both $d = 2$ and 3. It is also worth noticing that for $d = 3$ the simple theory presented in this section allows to predict the critical point of site percolation ($k = 1$) with the accuracy of $\approx 0.2\%$ using only the information available for the continuous percolation.

Encouraged by the success of the theory for $d = 2, 3$, one might ask whether it can be applied in higher dimensions. Since $V_{\rm ex} = 2^d$ for continuous percolation and $V_{\rm ex} = 2d + 1$ for site percolation, equation (9) suggests a general relation between the critical porosity in the continuous ($k \to \infty$) and site ($k = 1$) percolation on regular lattices of arbitrary dimension d,

$$\varphi_1^{\rm c} \approx (\varphi_\infty^{\rm c})^{2^d/2d+1}. \tag{13}$$

This equation correctly predicts that $\varphi_1^{\rm c} < \varphi_\infty^{\rm c}$ for space dimensions 3 and higher. Moreover, using the available results for the high-dimensional site percolation [34] and continuous percolation of oriented hypercubes [9], it is straightforward to verify that for dimensions $d \leq 5$ the values of the site percolation threshold $1 - \varphi_1^{\rm c}$ predicted from (13) deviate from the correct ones by less than 3.5%, whereas for $6 \leq d \leq 11$ the accuracy varies erratically between 8 and 15%. One possible explanation is as follows. One might expect that the quality of our approach is very good for large k and worsens as k goes down to 1, especially for $k \leq k^{\max}$, i.e. behind the maximum value of $\varphi^{\rm c}(k)$. Since $k^{\max}$ diverges with d, the quality of (13), which involves the information for $k = 1$, can be expected to decline for large d. It is also possible that the smaller accuracy of (13) for $d \geq 6$ is related to 6 being the critical dimension for standard percolation [35].

4.4. Relation to the site percolation with complex neighborhood

Percolation of obstacles of linear size k can be mapped on the standard site percolation with complex neighborhood problem. Consider an example visualized in figure 8, which shows the simplest nontrivial case $d = 2$, $k = 2$. The position of each obstacle on the lattice can be identified by the coordinates of one of the elementary cells making up the obstacle, e.g., the one occupying the top leftmost corner. In figure 8 this characteristic elementary cell for the 2×2 obstacle drawn with a thick solid line is marked by a cross. Another obstacle is connected to the reference one if and only if its characteristic elementary cell is located in one of the elementary cells marked by circles in figure 8 (which form the "excluded volume" $V_{\rm ex}$ for the reference object). Thus, the connectedness of a group of squares of linear size $k = 2$ is equivalent to that of elementary squares of linear size 1 with complex neighborhood marked with circles. This observation can be generalized to arbitrary space dimension d, arbitrary value of k and even arbitrary obstacle shape.

While the connectedness in the two models is equivalent, the porosities in each model are different—in the site percolation with complex neighborhood each obstacle occupies only one elementary cell. The porosity in the equivalent problem of site percolation, denoted henceforth by π, can be calculated from (1) with $v = 1$. This immediately leads to

$$\varphi_k^{\rm c} = (\pi_k^{\rm c})^{k^d}, \tag{14}$$

where $\pi_k^{\rm c}$ is the critical porosity in the equivalent site percolation with complex neighborhood problem.

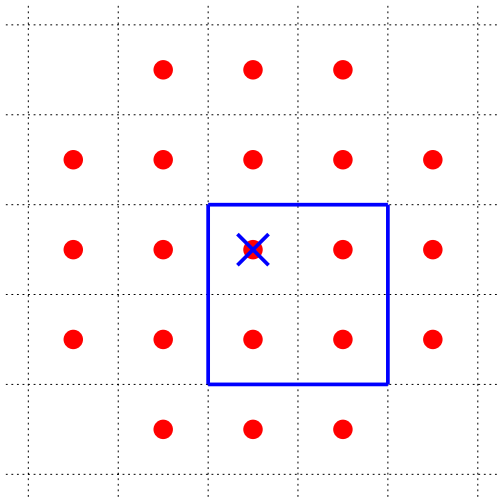

Figure 8. (Color online) The relation between percolation of squares of size $k \times k$ and the standard site percolation with complex neighborhood. See the text for detailed explanation.

The site percolation with complex neighborhood corresponding to the case illustrated in figure 8 ($d = 2$, $k = 2$) was investigated by Majewski and Malarz [36], who found $1 - \pi_2^{\mathrm{c}} \approx 0.196$. This is consistent with our result $1 - \pi_2^{\mathrm{c}} = 0.196724(5)$ that follows from (14) and the value of $\varphi_2^{\mathrm{c}} = 0.41635(2)$ listed in table 1.

5. Conclusions and outlook

The model of overlapping hypercubes, besides its applications in porous media modelling, allows one to investigate the transition between discrete and continuous percolation. We developed a simple phenomenological theory, an extension of the excluded volume approximation to discrete systems, which describes this transition with a remarkable accuracy. We verified this theory numerically in dimensions 2 and 3 and gave evidence that it is likely to remain valid in higher dimensions. We were also able to improve the accuracy of the determination of the continuous percolation threshold of aligned, overlapping cubes in three dimensions as well as to provide the values of continuous percolation thresholds of the void space around aligned squares and cubes in dimensions two and three. Moreover, we showed that a direct relation between the model of overlapping objects of arbitrary shape and the standard site percolation with complex neighborhood can be used to improve the accuracy of the percolation threshold determination in a class of percolation models.

We found that the percolation threshold in a model of aligned, overlapping squares or cubes randomly distributed on a regular lattice is a nonmonotonic function of their

size. This is an unexpected behavior, potentially affecting porous media modelling. Percolation of the void space around squares or cubes turns out to behave in a more regular way, as in this case the critical porosity can be approximated by a function linear in the reciprocal of the obstacle linear size.

Universality of the results presented here requires further studies, especially on obstacles of needle-like shapes, an idea that proved illuminating for the development of the excluded volume theory [16, 17, 11, 27].

References

[1] Salvatore Torquato. *Random heterogeneous materials: microstructure and macroscopic properties*. Springer, New York, 2002.

[2] Harold L. Weissberg. Effective diffusion coefficient in porous media. *J. Appl. Phys.*, 34(9):2636–2339, 1963.

[3] J. C. Maxwell. *A Treatise on Electricity and Magnetism*, volume I. Clarendon Press, London, 2 edition, 1881.

[4] Mikko Voutilainen, Paul Sardini, Marja Siitari-Kauppi, Pekka Kek+l+inen, Vesa Aho, Markko Myllys, and Jussi Timonen. Diffusion of tracer in altered tonalite: Experiments and simulations with heterogeneous distribution of porosity. *Transport in Porous Media*, 96(2):319–336, 2013.

[5] J. M. Zalc, S. Reyes, and E. Iglesia. Monte-Carlo simulations of surface and gas phase diffusion in complex porous structures. *Chemical Engineering Science*, 58(20):4605 – 4617, 2003.

[6] Olivier Mace and James Wei. Diffusion in random particle models for hydrodemetalation catalysts. *Industrial & Engineering Chemistry Research*, 30(5):909–918, 1991.

[7] Don R. Baker, Gerald Paul, Sameet Sreenivasan, and H. Eugene Stanley. Continuum percolation threshold for interpenetrating squares and cubes. *Phys. Rev. E*, 66:046136, Oct 2002.

[8] S. Torquato. Effect of dimensionality on the continuum percolation of overlapping hyperspheres and hypercubes. *J. Chem. Phys.*, 136:054106, Oct 2012.

[9] S. Torquato and Y. Jiao. Effect of dimensionality on the continuum percolation of overlapping hyperspheres and hypercubes. II. Simulation results and analyses. *The Journal of Chemical Physics*, 137(7):074106, 2012.

[10] E. J. Garboczi, M. F. Thorpe, M. S. DeVries, and A. R. Day. Universal conductivity curve for a plane containing random holes. *Phys. Rev. A*, 43:6473–6482, Jun 1991.

[11] J. Asikainen and T. Ala-Nissila. Percolation and spatial correlations in a two-dimensional continuum deposition model. *Phys. Rev. E*, 61:5002–5008, May 2000.

[12] Christian D. Lorenz and Robert M. Ziff. Precise determination of the critical percolation threshold for the three-dimensional "Swiss cheese" model using a growth algorithm. *J. Chem. Phys.*, 114:3659, Feb 2001.

[13] D. J. Priour. Percolation through voids around overlapping spheres: A dynamically based finite-size scaling analysis. *Phys. Rev. E*, 89:012148, Jan 2014.

[14] S. C. van der Marck. Network approach to void percolation in a pack of unequal spheres. *Phys. Rev. Lett.*, 77:1785–1788, Aug 1996.

[15] A. Okazaki, K. Maruyama, K. Okumura, Y. Hasegawa, and S. Miyazima. Critical exponents of a two-dimensional continuum percolation system. *Phys. Rev. E*, 54:3389–3392, Oct 1996.

[16] I. Balberg. Recent developments in continuum percolation. *Philosophical Magazine Part B*, 56(6):991–1003, 1987.

[17] N Provatas, M Haataja, J Asikainen, S Majaniemi, M Alava, and T Ala-Nissila. Fiber deposition models in two and three spatial dimensions. *Colloids and Surfaces A: Physicochemical and Engineering Aspects*, 165:209 – 229, 2000.

[18] Stephan Mertens and Cristopher Moore. Continuum percolation thresholds in two dimensions. *Phys. Rev. E*, 86:061109, Dec 2012.

[19] W. Xia and M. F. Thorpe. Percolation properties of random ellipses. *Phys. Rev. A*, 38:2650–2656, Sep 1988.

[20] Y. B. Yi. Void percolation and conduction of overlapping ellipsoids. *Phys. Rev. E*, 74:031112, Sep 2006.

[21] M. Kohout, A.P. Collier, and F. Štěpánek. Effective thermal conductivity of wet particle assemblies. *International Journal of Heat and Mass Transfer*, 47(25):5565 – 5574, 2004.

[22] Maciej Matyka, Zbigniew Koza, Jarosław Gołembiewski, Marcin Kostur, and Michał Januszewski. Anisotropy of flow in stochastically generated porous media. *Phys. Rev. E*, 88:023018, Aug 2013.

[23] A. Koponen, M. Kataja, and J. Timonen. Tortuous flow in porous media. *Phys. Rev. E*, 54:406–410, Jul 1996.

[24] A. Koponen, M. Kataja, and J. Timonen. Permeability and effective porosity of porous media. *Phys. Rev. E*, 56:3319–3325, Sep 1997.

[25] Maciej Matyka, Arzhang Khalili, and Zbigniew Koza. Tortuosity-porosity relation in porous media flow. *Phys. Rev. E*, 78:026306, Aug 2008.

[26] Fangming Jiang and Antonio C.M. Sousa. Smoothed particle hydrodynamics modeling of transverse flow in randomly aligned fibrous porous media. *Transport in Porous Media*, 75(1):17–33, 2008.

[27] I. Balberg, C. H. Anderson, S. Alexander, and N. Wagner. Excluded volume and its relation to the onset of percolation. *Phys. Rev. B*, 30:3933–3943, Oct 1984.

[28] D. Stauffer and A. Aharony. *Introduction to Percolation Theory*. Taylor and Francis, London, 2 edition, 1994.

[29] M. B. Isichenko. Percolation, statistical topography, and transport in random media. *Rev. Mod. Phys.*, 64:961–1043, Oct 1992.

[30] V. Cornette, A.J. Ramirez-Pastor, and F. Nieto. Percolation of polyatomic species on a square lattice. *The European Physical Journal B – Condensed Matter and Complex Systems*, 36:391–399, Dec 2003.

[31] Xiao Xu, Junfeng Wang, Jian-Ping Lv, and Youjin Deng. Simultaneous analysis of three-dimensional percolation models. *Frontiers of Physics*, 9(1):113–119, 2014.

[32] Junfeng Wang, Zongzheng Zhou, Wei Zhang, Timothy M. Garoni, and Youjin Deng. Bond and site percolation in three dimensions. *Phys. Rev. E*, 87:052107, May 2013.

[33] Jesper Lykke Jacobsen. High-precision percolation thresholds and Potts-model critical manifolds from graph polynomials. *Journal of Physics A: Mathematical and Theoretical*, 47(13):135001, 2014.

[34] Peter Grassberger. Critical percolation in high dimensions. *Phys. Rev. E*, 67:036101, Mar 2003.

[35] J. W. Essam. Percolation theory. *Reports on Progress in Physics*, 43(7):833, 1980.

[36] M. Majewski and K. Malarz. Square lattice site percolation thresholds for complex neighbourhoods. *Acta Physica Polonica B*, 38:2191, June 2007.